Are Halide···Halide Contacts a Feature of Rock-Salts Only?

Yulia V. Nelyubina, Mikhail Yu. Antipin, and Konstantin A. Lyssenko*

A.N. Nesmeyanov Institute of Organoelement Compounds, Russian Academy of Sciences, 119991, Vavilov Street, 29, Moscow, Russia

Received: September 16, 2006; In Final Form: November 14, 2006

The electron density distribution function in the crystalline hydroxylammonium chloride obtained using the high-resolution X-ray diffraction technique was analyzed by means of Bader's "atoms in molecule" theory. The anion−anion interactions in the crystal of this ionic material were examined and the energy of the $Cl^-\cdots Cl^-$ contacts was estimated on the basis of the experimental data. The results obtained coincide well with the theoretical calculations and the X-ray diffraction data for the rock-salts. The existence of such type of interactions was shown to be not the unique feature of inorganic salts with point charge cations.

Introduction

The X-ray diffraction (XRD) analysis gives an opportunity to provide insight into the bonding peculiarities of the solid state and hence to understand how to handle the arrangement of molecules or ions to obtain materials with specific physical and chemical properties.[1] The main problem is that in many cases it is difficult to divide forced and attractive (bonding) interactions in crystal. For example, in crystalline salts with point charge ions, the predominant contacts are supposed to be cation−anion ones due to electrostatic reasons. However, according to some investigations in this field, rare anion−anion contacts were also detected in high-quality measurements of inorganic salts (see ref 2 and references therein).

For the ionic materials, a simple ratio of cation to anion radii correctly predicts the existence of halide−halide contacts in the alkaline halide crystals.[3] Apparently, this radius ratio criterion fails to provide the satisfactory description of the systems with bulky cations which cannot be approximated by the rigid ion model.

In accordance with the above the behavior of anions in the crystal with non-point charge cations is the point of interest. One of the most successful approaches to detecting intermolecular interactions is topological analysis of the electron density distribution function $\rho(\mathbf{r})$ derived from the high-resolution X-ray diffraction (XRD) data[4] by means of Bader's "atoms in Molecule" (AIM) theory.[5] Using the AIM formalism in conjunction with accurate XRD experiment, one can distinguish the binding interactions from all other contacts. This approach provides excellent results for minerals, molecular and ionic crystal structures.[4] Its additional advantage is the unique opportunity to estimate the energy of the interatomic contacts (E_{cont}) on the basis of the potential energy density function $v(r)$ value[6] in the corresponding bond critical point CP (3,−1) and even predict with high accuracy the sublimation enthalpy.[7]

Bader's analysis of experimental and theoretical electron densities of alkaline halides has been done in ref 8 The above anion−anion bonds were found in the crystals of LiF and NaF. On the other hand, in the case of NaCl, the CP (3,−1) for the Cl···Cl contact was observed only in the theoretical calculation, whereas it was not found in the experimental $\rho(\mathbf{r})$. In addition, the anion−anion interactions were reported for O···O contacts in MgO[10] and danburite ($CaB_2Si_2O_8$).[2] It is also noteworthy that recently, the application of the AIM concept to crystalline solids gave rise to the method, which affords the possibility to make structure prediction based upon topological radii of ions.[9] It was demonstrated that an anion to cation ratio (r_a/r_c) plays a key role in the determination of the topology of the rock-salt and the cesium chloride phases, i.e., the anion−anion contacts would happen only if r_a/r_c value (under assumption the ions as rigid spheres) is about 1.4 for the cesium chloride phase and 2.4 for the rock-salt one.

Accordingly, it was intriguing to check the occurrence of the halide···halide interactions in the crystal with non-point charge cations participating in formation of numerous directional contacts in which the anion−anion separation is comparable with that of alkaline halide. Therefore, in the present work, we report the results of the electron density analysis of hydroxylammonium chloride (**1**) by means of Bader's AIM theory on the basis of the high-resolution XRD data.

Experimental Section

The details of the X-ray data collection and conventional full-matrix anisotropic−isotropic refinement are listed in Table 1. The multipole refinement was carried out within the Hansen−Coppens formalism[11] using XD program package[12] with the core and valence electron density derived from wave functions fitted to a relativistic Dirac−Fock solution.[13] Before refinement, the N−H and O−H bond distances were normalized to the values obtained from the neutron data.[14] The level of multipole expansion was hexadecapole for chlorine and octupole for nitrogen and oxygen atoms. The dipole D_{10} and the hexadecapoles H_{40} were refined for all hydrogen atoms for more accurate description of hydrogen bonds.[12] All bonded pairs of atoms satisfy the Hirshfeld rigid-bond criteria (difference of the mean square displacement amplitude N(1)−O(1) was $2\cdot10^{-4}$ Å^2). The residual electron density was not more that 0.12 eÅ^{-3}. Analysis of the $\rho(\mathbf{r})$ function topology was carried out using the WINXPRO program package.[15] The results of the multipole refinement are also listed in Table 1.

DFT calculations of the hydroxylammonium cation in the Cs symmetry were performed with the Gaussian98 program package[16] at the B3LYP level using the 6-311+G** basis set. The

* Corresponding author. E-mail: kostya@xrlab.ineos.ac.ru.

10.1021/jp066049u CCC: $37.00
Published on Web 01/24/2007

TABLE 1: Details of Data Collection and Refinement of 1

	NH_3OHCl
M	69.49
T	100 K
space group	$P2_1/n$
a, Å	6.8955(5)
b, Å	5.9218(5)
c, Å	7.2123(5)
β, deg	114.141(5)
V, Å^3	268.75(4)
Z	4
density, g cm^{-3}	1.718
F(000)	144
μ (MoKα), cm^{-1}	10.9
diffractometer	Bruker AXS SMART APEX2
absorption correction (MoKα)	semiempirical from equivalents
scan technique	ω-scan with 0.5° step in ω
θ_{max}, deg	50
number of measured refl.	13121
number of independent refl. (R(int))	2818 (0.0246)
number of observed refl. with $I > 2\sigma(I)$	2416
conventional refinement	
wR2	0.0448
R1 calculated against F	0.0176
GOF	1.000
ρ_{max}/ρ_{min}, e Å^{-3}	0.326/−0.373
multipole refinement	
number of rfln. with $I > 3\sigma(I)$	2392
R1 calculated against F	0.0149
Rw calculated against F	0.0123
GOF	0.85
ρ_{max}/ρ_{min}, e Å^{-3}	0.119/−0.107

optimization was followed by the evaluation of the harmonic vibration frequencies.

Results and Discussion

The geometry of the cation in the crystal of **1** is almost the same as that in isolated state with the N(1)−O(1) bond length equal to 1.4114(4) and 1.4060 Å for the XRD and DFT data, respectively. In spite of numerous hydrogen bonds formed (see below), the antiperiplanar disposition of the H(1O) and H(3N) atoms persists in the crystal with torsion H(1O)−O(1)−N(1)−H(3N) angle equal to 175°.

Analysis of the crystal packing in **1** shows that the cations are assembled into infinite chains by the O(1)···H(1N)−N(1) H-bonds with the O···N distance equal to 2.9780(4) Å. The chains are hold together by the Cl···H−N and Cl···H−O contacts forming the three-dimensional framework. These cation−anion interactions are characterized by comparatively high values of the Cl···N and Cl···O distances varying in the range of 3.0321(5)−3.2143(5) Å. In contrast to pure ionic crystals, the Cl···H−N/Cl···H−O angles are nearly linear and equal to 156(1)−164(1)°. The additional Cl···O and Cl···N contacts (the values of the Cl···O−N and Cl···N−O angles are 172 and 167°, respectively) observed in **1** probably play the same role in the formation of crystal packing (Figure 1). Since these interactions do not influence significantly on the geometry of the cation (the N(1)−O(1) bond lengths in the condensed and gaseous phases vary slightly), one can expect them being considerably weak.

Due to the above intermolecular contacts, chlorine anions are located at relatively short distance of 3.8053(5) and 3.9046(5) Å. Both values are even smaller than that of Cl$^-$···Cl$^-$ separation in NaCl (3.981 Å).[8] It is noticeable that the formation of such Cl···Cl contacts is not the unique feature of **1**. We found at least 134 organic compounds in the Cambridge Structural Database (CSD) with a Cl···Cl separation in the range of 3.6−3.9 Å. Moreover, in 76 structures the Cl···Cl distance is less than the sum of van der Waals radii for chlorine (3.8 Å). Therefore, one can question whether or not the interatomic "contacts" in the crystal of **1** correspond to attractive interactions. To accomplish this the topological analysis of the electron density distribution function $\rho(\mathbf{r})$ in **1** was performed.

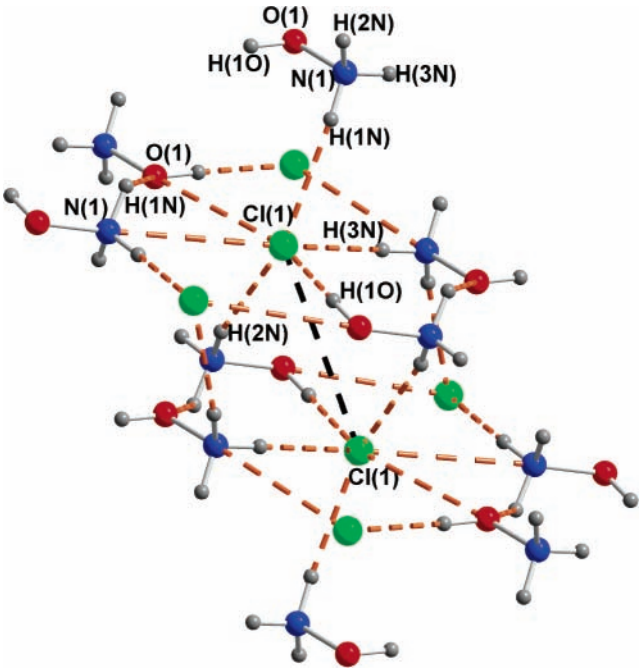

Figure 1. The fragment of the crystal packing of **1**.

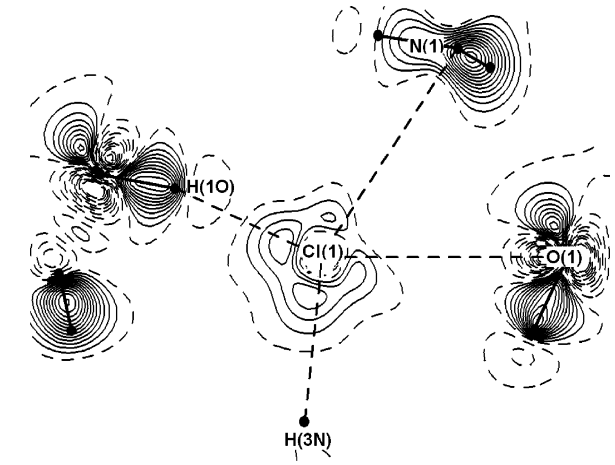

Figure 2. The experimental DED distribution in the section of square-planar surrounding of chloride anion in the crystal of **1**. The contours are drawn with 0.05 e/Å^{-3} step; the negative ones are dashed.

Electron Density Distribution. The deformation electron density (DED) distribution in **1** (Figure 2) is characterized by expected features: the accumulation of DED in the interatomic area and several maxima in the vicinity of the Cl(1) ion corresponding to four localized electron pairs (LP) of chloride anion. The mutual disposition of the chloride LPs according to the analysis of $-\nabla^2\rho(\mathbf{r})$ function topology can be described as the significantly distorted (flattened) tetrahedron. This is the direct consequence of the crystal packing effects, i.e., the influence of the distorted square-planar surrounding of Cl$^-$ anion formed by two nitrogen and two oxygen atoms (Figure 1).

To investigate the peculiarities of charge distribution in the crystal of **1**, we determined the atomic basins (Ω) surrounded by zero-flux surface and integrated $\rho(\mathbf{r})$ over Ω to obtain

TABLE 2: Atomic Charges, Volumes and Lagrangian for Atoms in 1

	q, e	V_{at}, Å^3	$L(r)$, 10^{-4} a.u.
Cl(1)	−0.28	27.91	1.22
O(1)	−0.69	15.04	1.02
H(1O)	0.54	2.26	1.19
N(1)	−0.96	13.34	4.07
H(1N)	0.48	2.7	1.16
H(2N)	0.42	3.16	0.33
H(3N)	0.49	2.51	0.57

TABLE 3: Topological Parameters of the $\rho(\mathbf{r})$ Function in the CPs (3, −1) for the Cation−Anion and Cation−Cation Interactions in the Crystal of 1

interaction	R, Å	$\rho(\mathbf{r})$, e Å^{-3}	$\nabla^2\rho(\mathbf{r})$, e Å^{-5}	$v(r)$, a.u.	E_{cont}, kcal/mol
Cl(1)···H(1N)	2.208	0.122(1)	1.99(1)	0.014033	4.40
Cl(1)H(2N)[a]	2.224	0.137(1)	1.83(1)	0.01503	4.72
Cl(1)···H(3N)[b]	2.199	0.142(1)	1.5(1)	0.014348	4.50
O(1)···H(1N)[c]	2.551	0.065(1)	1.19(1)	0.006583	2.07
Cl(1)···H(1O)[d]	2.079	0.16(1)	2.84(1)	0.021101	6.62
Cl(1)···N(1)[e]	3.1722(5)	0.067(1)	0.67(2)	0.00499	1.57
Cl(1)···O(1)[f]	3.1163(5)	0.06(1)	0.81(2)	0.004974	1.56

[a] The atom was obtained from basic one by the symmetry operation x −1/2, $-y+3/2$, $z+1/2$. [b] $-x+1$, $-y+2$, $-z$. [c] $x-1/2$, $-y+3/2$, $z-1/2$. [d] $x+3/2$, $y-1/2$, $-z+1/2$. [e] $-x+5/2$, $y-3/2$, $-z+1/2$. [f] $-x+1$, $-y+1$, $-z$.

basins's electron populations and thus atomic charges. Although the integrated Langrangian ($L(r) = -1/4\nabla^2\rho(\mathbf{r})$) for every Ω has to be exactly zero,[5] a reasonably small numbers with averaged value of $1.4\cdot10^{-4}$ a.u. with maximum $L(r)$ observed for N(1) atom ($4.1\cdot10^{-4}$ a.u.) were obtained. The values of atomic charges indicate the high degree of charge transfer (0.72e) from the chloride anion to the bulky cation (Table 2), unlike in the pure ionic compounds where the corresponding parameters are approximately those of free ions.[2] This difference is mainly due to the presence of Cl$^-$···H−O and Cl$^-$···H−N hydrogen bonds of intermediate strength in the crystal of **1**, whereas in the case of inorganic salts all of the binding interactions are electrostatic (see ref 17 and references therein).

Another important point in the context of ionic materials is the concept of atomic size. Therefore, in addition to the atomic charges in the crystal of **1**, we also estimated atomic volumes according to the above procedure. Since the integration was carried out numerically, it is important to indicate that their sum in the crystal (66.92 Å^3) reproduces well the unit cell volume per molecule (67.19 Å^3) with the relative error 0.04%. The expected relationship was found on comparing the cationic and anionic volumes, i.e., the cation to the chloride anion ratio is larger than 1.3.

The atomic parameters for the different hydrogens of the NH_3 group vary only slightly (see Table 2). Indeed, the H(2N) atom charge is 0.42 e, while the corresponding values for H(1N) and N(3N) ones are approximately the same and equal to 0.48 and 0.49 e, respectively The similar tendency is observed for their volumes.

With this fact in mind, one can relate the observed variation of H-atoms volumes and charges in the crystal of **1** to the different "H-bonding graphs" formed by these hydrogens. We therefore performed the search for bond critical points in the area of the expected contacts. Accordingly, the CPs (3,−1) corresponding to the Cl$^-$···H−N/Cl$^-$···H−O and O···H−N H-bonds and the other interionic contacts were localized, and their energy was estimated on the basis of the Espinosa's correlation scheme[6] (Table 3)—the semiquantitive relationship between the energy of the contact (E_{cont}) and the value of the potential energy density function $v(r)$ in the CP (3,−1). Thus the Cl(1)···H(2N) interaction (E_{cont} = 4.72 kcal/mol) was found to be the strongest within all of the Cl$^-$···H−N bonds (E_{cont} is equal to 4.40 and 4.50 kcal/mol for the H(1N) and H(3N) hydrogens). This agrees well with the above comparison of hydrogen charges and volumes.

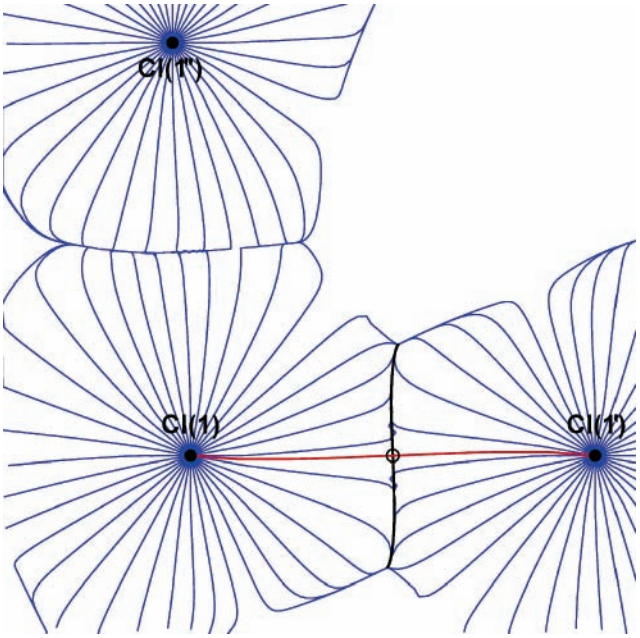

Figure 3. The molecular graph in the section of chlorine···chlorine contact in the crystal of **1**. The Cl(1′) and Cl(1″) atoms were obtained from the basis one by the symmetry operation $-x$, $-y$, $-z$ (center of inversion) and $1+x$, $1+y$, $1+z$ (translation), respectively (the values of the Cl(1)···Cl(1′) and Cl(1)···Cl(1″) separation are equal to 3.8053(5) and 3.9051(5) Å). The atom surface is drawn by a black line; the bond path by a red one and the black circle marks the CP (3, −1).

It appears from the above peculiarities of crystal packing that the presence of numerous directional cation−anion as well as the cation−cation interactions makes the structure **1** quite different from the pure ionic one, which is observed, for example, in the case of the NaCl. Therefore, it is interesting to examine the occurrence of Cl$^-$···Cl$^-$ contacts in the crystal of **1** and to perform the comparative analysis of their topological characteristics derived from XRD data of **1** and theoretical investigations of the alkaline halides reported in literature.[8,9]

Although the validity of analysis of the $\rho(\mathbf{r})$ within the AIM theory for weak interactions has been debated,[18] the comparison of the topology for the experimental and theoretical $\rho(\mathbf{r})$ and potential energy density distribution $v(r)$ functions has resolved this controversy.[19,20] Bader has demonstrated that each bond path in the electron density is mirrored by the virial path, a line of maximum potential energy density, which in turn indicates that the presence of the bond path or critical point (3,−1) between the pair of atoms in question is the "universal indicator of bonding between atoms".[19]

Cl$^-$···Cl$^-$ Interaction. The CP (3,−1) and its associated bond path in the experimental electron density for the anion−anion contact are shown in Figure 3. It should be noted that although the shortest chlorine···chlorine distances are sufficiently close to each other (see above), only anions related by center of symmetry with the separation of 3.8053(5) Å participate in the Cl$^-$···Cl$^-$ interaction. In addition to the CPs (3,−1) for the above contacts we have located a number of ring CPs (3,+1) and cage CPs (3,+3) caused by the three-dimensional framework. The characteristic set of critical points satisfies the Morse equation.[5]

TABLE 4: Selected Topological Characteristics of the Experimental and Model Electron Densities in the CP (3, −1) for the $Cl^-\cdots Cl^-$ Contact in the Crystal of 1 and Crystal of NaF[8] and NaCl[9]

	$\rho(r)$, eÅ^{-3}	$\nabla^2\rho(r)$, eÅ^{-5}	v(r), a.u.	$h_e(r)$, a.u.	λ_1, e Å^{-5}	λ_2, e Å^{-5}	λ_3, e Å^{-5}
experimental ρ(r)	0.033(1)	0.37(2)	0.002123	0.000879	−0.086	−0.061	0.522
model ρ(r)	0.029	0.36	0.001909	0.000914	−0.046	−0.020	0.426
NaF	0.03(1)	0.39(2)	n/a	n/a	−0.07	−0.02	0.48
NaCl	0.07	0.30	n/a	n/a	n/a	n/a	n/a

This is in a good agreement with the fact that only one of the $Cl^-\cdots Cl^-$ pairs displays a bond CP.

To demonstrate that the occurrence of anion−anion interactions is not entirely the consequence of the charges redistribution due to the formation of chemical bonds, we also performed topological analysis of the model $\rho(\mathbf{r})$ composed only from noninteracting overlapping spherical atoms (pro-crystal). The values of the $\rho(\mathbf{r})$, $\nabla^2\rho(\mathbf{r})$ functions and Hessian matrix eigenvalues (Table 4) of both electron density functions in this bond CP agree very well with the experimental data for NaF and the theoretical results for NaCl.[8,9] Furthermore, topological analysis of the potential energy density function $-v(r)$ in **1** also revealed the presence of the CP (3,−1) located in the same position between two chloride anions as the corresponding CP (3,−1) in the $\rho(\mathbf{r})$.

It should be mentioned that the X−Cl(2)···Cl(1) contacts (X = any bonded atom, e.g., C) in general are attributed to the charge transfer from the LP of Cl(1) to the σ*-orbital of the X−Cl(2) bond.[21,22] In terms of electron localization function (ELF)[23,24] or $\nabla^2\rho(\mathbf{r})$, the manifestation of such type of interactions is that the LP of one atom is directed toward the area of electron density depletion for the other one ("peak to hole" type). However, the analysis of experimental ELF,[23] which provides the reliable information about the disposition of LPs,[23,24] shows that the $Cl^-\cdots Cl^-$ interactions in the crystal of **1** correspond neither to "peak to hole" as in solid Cl_2[21,23] and ClF[22] nor to "peak to peak" type. As follows from Figure 4 the lines connecting maxima (LP) with nucleus for interacting ions are tilt from the interatomic line (by ca. 30°) and parallel to each other.

The values of $\nabla^2\rho(\mathbf{r})$ at CP (3,−1) can be used as a measure of the local accumulation of the charge density. Thus, the positive Laplacian as well as local energy density $h_e(\mathbf{r})$ for the anion−anion interactions in **1** indicates that they are of the closed-shell type with the absolute values of $\nabla^2\rho(\mathbf{r})$ being smaller than in the case of the H-bonds and comparable with those for Cl···O and Cl···N contacts (Table 3).

The energy of this $Cl^-\cdots Cl^-$ contact estimated on the basis of the v(r) value is equal to 0.67 and 0.60 kcal/mol for the crystal and pro-crystal of **1**, respectively (Table 4), that is extremely small as compared with those for the Y−H···Cl^- (Y═N, O) hydrogen bonds (E_{cont} = 1.5 − 2.84 kcal/mol). In other words, there is the evidence that the considerably strong cation−anion interactions determine the crystal pattern of **1** resulting in the formation of the weak anion−anion contacts.

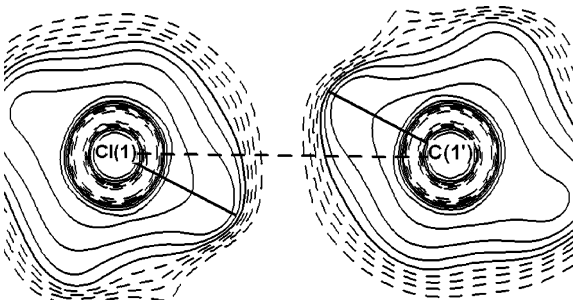

Figure 4. ELF in the section of anion−anion contact in the crystal of **1**. The contours are drawn with 0.1 step; the ones with ELF < 0.5 are dashed. The contour of ELF equal to 0.5 is drawn by a thicker line.

Conclusion

Topological analysis of the electron density distribution in the crystal of **1** indicates that the anion−anion interactions are not only "privilege" of pure ionic salts with point charge ions but also the case of rather bulky cation such as hydroxylammonium. At the same time, the data obtained revealed that the presence of bonding path is not solely a consequence of Cl···Cl interatomic separation. Thus, one cannot be sure that chloride···chloride interactions are observed in all of the mentioned 76 crystal structures with shortened Cl···Cl contacts. However, the result of present investigation clearly shows that we also cannot exclude them basing on "chemical common sense." Finally, although the described interactions are extremely weak as compared with the cation−anion ones the detailed investigations of the anion−anion supramolecular aggregations can probably serve as "auxiliary basis" for anion recognition.

Acknowledgment. This study was financially supported by the Russian Foundation for Basic Research (Project 06-03-32557), the Foundation of the President of the Russian Federation (Federal Program for the Support of Leading Scientific Schools, Grant NSh 1060.2003.30, and Young Doctors, Grant MK-1054.2005.3), and the Russian Science Support Foundation.

Supporting Information Available: Crystallographic data in cif format. This material is available free of charge via the Internet at http://pubs.acs.org.

References and Notes

(1) Brammer, L. *Chem. Soc. Rev.* **2004**, *33*, 476. Braga, D.; Brammer, L.; Champness, N. R. *Cryst. Eng. Comm.* **2005**, *7*, 1. Kitagawa, S.; Kitaura, R.; Noro, S. *Angew. Chem., Int. Ed.* **2004**, *43*, 1466. Rao, C. N. R.; Natarajan, S.; Vaidhyanathan, R. *Angew. Chem., Int. Ed.* **2004**, *43*, 2334. Krishnamohan Sharma, C. V. *Cryst. Growth Des.* **2002**, *6*, 465.

(2) Lua˜na, V.; Costales, A.; Mori-Sánchez, P.; Pendás, A. M. *J. Phys. Chem.* **2003**, *107*, 4912.

(3) Pauling, L. J. *J. Am. Chem. Soc.* **1929**, *51*, 1010.

(4) Koritsanszky, T. S.; Coppens, P. *Chem. Rev.* **2001**, *101*, 1583. Gatti, C.; *Z. Kristallogr*. **2005**, *220*, 399. Tsirelson, V. G.; Ozerov, R. P. *Electron Density and Bonding in Crystals: Principles, Theory and X-Ray Diffraction Experiments in Solid State Physics And Chemistry*; IOP Publishing Ltd.: 1996.

(5) Bader, R. F. W. *Atoms in molecules. A quantum theory*; Clarendron Press: Oxford, 1990.

(6) Espinosa, E.; Molins, E.; Lecomte, C. *Chem. Phys. Lett.* **1998**, *285*, 170. Espinosa, E.; Alkorta, I.; Rozas, I.; Elguero, J.; Molins, E. *Chem. Phys. Lett.* **2001**, *336*, 457.

(7) Lyssenko, K. A.; Korlyukov, A. A.; Golovanov, D. G.; Ketkov, S. Yu.; Antipin, M. Yu. *J. Phys. Chem.* **2006**, *A110*, 6545. Glukhov, I. V.; Lyssenko, K. A.; Korlyukov, A. A.; Antipin, M. Yu. *Russ. Chem. Bull. Int. Ed.* **2005**, *54*, 547. Lyssenko; K. A.; Korlyukov; A. A.; Antipin, M. Yu. *Mendeleev Commun.* **2005**, *90*.

(8) Tsirelson, V.; Abramov, Yu.; Zavodnik, V.; Stash, A.; Belokoneva, E.; Stahn, J.; Pietsch, U.; Feil, D. *Struct. Chem.* **1998**, *9*, 249.

(9) Pendás, A. M.; Costales, A.; Lua˜na, V. *J. Phys. Chem.* **1998**, *102*, 6937.

(10) Tsirelson, V.; Avilov, A. S.; Lepeshov, G. G.; Kulygin, A. K.; Stahn, J.; Pietsch, U.; Spence, J. C. H. *J. Phys. Chem.* **2001**, *105*, 5068.

(11) Hansen, N. K.; Coppens, P. *Acta Crystallogr.* **1978**, *A34*, 909.
(12) Koritsansky, T. S.; Howard, S. T.; Richter, T.; Macchi, P.; Volkov, A; Gatti, C.; Mallinson, P. R.; Farrugia, L. J.; Su, Z.; Hansen, N. K. *XD - A Computer Program Package for Multipole Refinement and Topological Analysis f Charge Densities from Diffraction Data*; 2003.
(13) Su, Z.; Hansen, N. K. *Acta Crystallogr.* **1998**, *A54*, 646.
(14) Padmanabhan, V. M.; Smith, H. G.; Peterson, W. *Acta Crystallogr.* **1967**, *22*, 928.
(15) Stash, A.; Tsirelson, V. *WinXrpo, A Program for Calculation of the Crystal and Molecular Properties Using the Model Electron Density*; 2001 (further information available at http://xray.nifhi.ru/wxp/). Stash, A.; Tsirelson, V. J. *Acta Crystallogr.* **2002**, *35*, 371.
(16) Frisch, M. J.; Trucks, G. W.; Schlegel, H. B.; Scuseria, G. E.; Robb, M. A.; Cheeseman, J. R.; Zakrzewski, V. G.; Montgomery, J. A., Jr.; Stratmann, R. E.; Burant, J. C.; Dapprich, S.; Millam, J. M.; Daniels, A. D.; Kudin, K. N.; Strain, M. C.; Farkas, O.; Tomasi, J.; Barone, V.; Cossi, M.; Cammi, R.; Mennucci, B.; Pomelli, C.; Adamo, C.; Clifford, S.; Ochterski, J.; Petersson, G. A.; Ayala, P. Y.; Cui, Q.; Morokuma, K.; Malick, D. K.; Rabuck, A. D.; Raghavachari, K.; Foresman, J. B.; Cioslowski, J.; Ortiz, J. V.; Stefanov, B. B.; Liu, G.; Liashenko, A.; Piskorz, P.; Komaromi, I.; Gomperts, R.; Martin, R. L.; Fox, D. J.; Keith, T.; Al-Laham, M. A.; Peng, C. Y.; Nanayakkara, A.; Gonzalez, C.; Challacombe, M.; Gill, P. M. W.; Johnson, B. G.; Chen, W.; Wong, M. W.; Andres, J. L.; Head-Gordon, M.; Replogle, E. S.; Pople, J. A. *Gaussian 98*, Revision A.7; Gaussian, Inc.: Pittsburgh, PA, 1998.
(17) Meot-Ner, (Mautner), M. *Chem. Rev.* **2005**, *105*, 213.
(18) Cioslowski, J.; Mixon, S. T.; Edwards, W. D. *J. Am. Chem. Soc.* **1991**, *113*, 1083. Cioslowski, J.; O'Connor, P. B.; Fleischmann, E. D. J. *Am. Chem. Soc.* **1991**, *113*, 1086. Cioslowski, J.; Mixon, S. T. *J. Am. Chem. Soc.* **1992**, *114*, 4382. Cioslowski, J.; Ediginton, L.; Stefanov, B. B. *J. Am. Chem. Soc.* **1995**, *117*, 10381. Poater, J.; Sola, M.; Bickelhaupt, F. M. *Chem. Eur. J.* **2006**, *12*, 2889.
(19) Bader, R. F. W. *J. Chem. Phys. A* **1998**, *102*, 7314.
(20) Matta, C. F.; Hernández-Trujillo, J.; Tang, T.; Bader, R. *Chem. Eur. J.* **2003**, *9*, 1940. Zhurova, E. A; Tsirelson, V. G.; Stach, A. I.; Pinkerton, A. A. *J. Amer. Chem. Soc.* **2002**, *124*, 4574. Lyssenko, K. A.; Antipin, M. Yu.; Gurskii, M. E.; Bubnov, Yu. N.; Karionova, A. L.; Boese, R. *Chem. Phys. Lett.* **2004**, *384*, 40. Bader R. F. W.; De-Cai Fang *J. Chem. Theory Comput.* **2005**, *1*, 403.
(21) Tsirelson, V. G.; Zou, P. F.; Tang, T. H.; Bader, R. F. W. *Acta Crystallogr.* **1995**, *A51*, 143−153.
(22) Boese, R.; Boese, A. D.; Blaser, D.; Antipin, M. Yu.; Ellern, A.; Seppelt, K. *Angew. Chem., Int. Ed. Engl.* **1997**, *36*, 1489.
(23) Tsirelson, V.; Stash, A. *Chem. Phys. Lett.* **1998**, *285*, 170.
(24) Savin, A.; Nesper, R.; Wengert, S.; Fassler, T. *Angew. Chem., Int. Ed. Engl.* **1997**, *36*, 1809.